Radiation Impedance of an Array of Circular Capacitive Micromachined Ultrasonic Transducers

Muhammed N. Senlik, *Student Member, IEEE*, Selim Olcum, *Student Member, IEEE*, Hayrettin Köymen, *Senior Member, IEEE*, and Abdullah Atalar, *Fellow, IEEE*

***Abstract*—The radiation impedance of a capacitive micromachined ultrasonic transducer (cMUT) with a circular membrane is calculated analytically using its velocity profile for the frequencies up to its parallel resonance frequency for both the immersion and the airborne applications. The results are verified by finite element simulations. The work is extended to calculate the radiation impedance of an array of cMUT cells positioned in a hexagonal pattern. A higher radiation resistance improves the bandwidth as well as the efficiency of the cMUT. The radiation resistance is determined to be a strong function of the cell spacing. It is shown that a center-to-center cell spacing of 1.25 wavelengths maximizes the radiation resistance, if the membranes are not too thin. It is also found that excitation of nonsymmetric modes may reduce the radiation resistance in immersion applications.**

I. Introduction

Capacitive micromachined ultrasonic transducers (cMUTs) offer wider bandwidth in air [1]–[4] and in water [5]–[8] compared with their piezoelectric alternatives due to their low mechanical impedances. The limit for the bandwidth is the parallel resonance frequency of the cMUT membrane in water, whereas the mechanical impedance of the membrane limits the bandwidth in air. In this work, the acoustic loading on the circular cMUT membranes is investigated by calculating their radiation impedances.

The mechanical impedance of a cMUT membrane in vacuum is well studied [9]. It shows successive series and parallel resonances, where force and velocity become zero, respectively [10]. When a cMUT is immersed in water, the acoustic loading on the cell is high and results in a wide bandwidth. All mechanical resonance frequencies shift to lower values because of the imaginary part of the radiation impedance. If a cMUT is used in air, the radiation impedance is rather low, and the bandwidth is limited by the mechanical Q of the membrane. It is therefore preferable to increase the radiation resistance to get a higher bandwidth in airborne applications. In addition, for the same membrane motion, a higher acoustic power is delivered to the medium, if the radiation resistance is higher. Hence, a higher radiation resistance is desirable to be able to transmit more power, because the gap limits the maximum allowable membrane motion.

The efficiency of a transducer is defined as the ratio of the power radiated to the medium to the power input to the transducer [11]. The loss in a cMUT due to the electrical resistive effects and the mechanical power lost to the substrate can be represented as a series resistance [1]. Hence, the efficiency will increase if the radiation resistance increases in both airborne and immersion cMUTs, because a smaller portion of the energy will be dissipated on the loss mechanisms such as the coupling into the substrate.

There are several approaches to model the radiation impedance of the cMUT membrane. In [12], the radiation impedance is modeled using an equal size piston radiator. In [13], an equivalent piston radiator with the appropriate boundary conditions is defined and its radiation impedance is used. In [14], the radiation impedance of an array is modeled with lumped circuit elements. In [15], the radiation impedance is calculated by subtracting the mechanical impedance of the membrane from the input mechanical impedance as computed by a finite element simulation. In [16], cMUT is modeled with a modal expansion-based method, and the radiation impedance is calculated using that method. Caronti *et al.* [17] calculated the radiation impedance of an array of cells performing finite element simulations with a focus on the acoustic coupling between the cells.

The radiation impedance of an array of cMUT cells is not well known. In this work, the radiation impedance of an array of cMUT cells with circular membranes is presented. First, the radiation impedance of a single cMUT cell is calculated using its velocity profile. Then, the radiation impedance of array of cMUT cells is calculated from analytical expressions and compared with those found from finite element simulations.

II. Mechanical Behavior of a Circular cMUT Membrane

A. Finite Element Method (FEM) Simulations

FEM simulations are performed using ANSYS[1] (ANSYS Inc., Canonsburg, PA) in water [18]–[20] to calculate

Manuscript received January 30, 2009; accepted December 9, 2009. This work is supported in part by the Turkish Scientific and Research Council (TUBITAK) under project grants 105E23 and 107T921. S. Olcum acknowledges the support of TUBITAK and ASELSAN for their Ph.D. scholarship programs. A. Atalar thanks TUBA for the research support.

The authors are with the Electrical and Electronics Engineering Department, Bilkent University, Ankara, Turkey (e-mail: niyazi@ee.bilkent.edu.tr).

Digital Object Identifier 10.1109/TUFFC.2010.1501

[1]The membrane, the fluid, and the absorbing boundary are modeled using PLANE42, FLUID29, and FLUID129 elements, respectively.

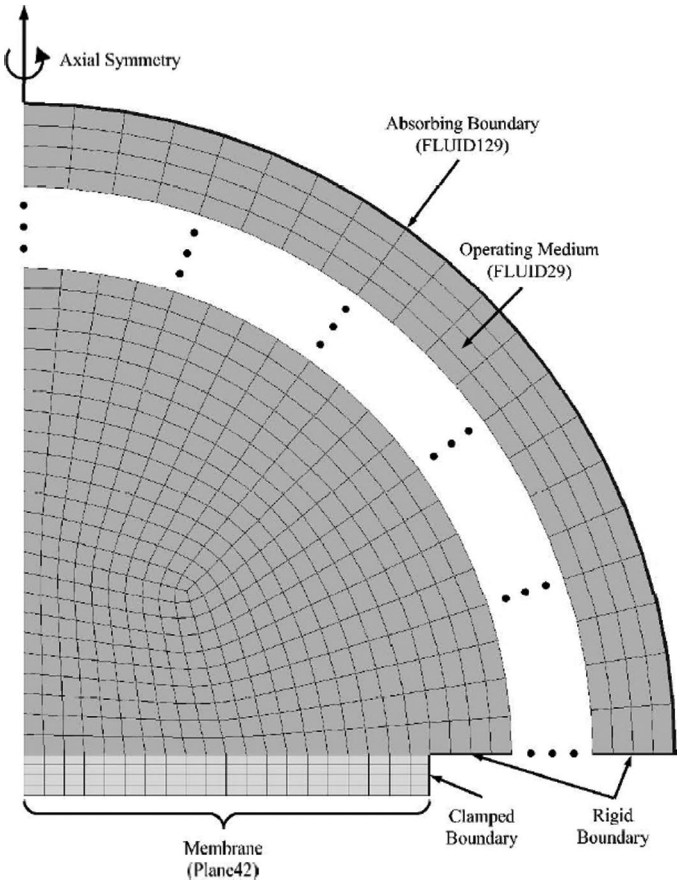

Fig. 1. Finite element (FE) model of a cMUT cell with the operating medium.

the velocity and the pressure profiles on the surface of the cMUT membrane. As indicated in Fig. 1, the absorbing boundary is $2\lambda_0$ away from the membrane at the lowest operating frequency and the mesh size is $\lambda_0/40$ at the highest operating frequency, where λ_0 is the wavelength in the operating medium. A rigid baffle is assumed. The material parameters used in the simulations can be found in Table I.

B. Velocity Profile

The velocity profile on the surface of a circular radiator can be expressed analytically using a linear combination of functions given by [21]–[23]

$$v_n(r) = V_{rms}\sqrt{2n+1}\left(1-\frac{r^2}{a^2}\right)^n U(a-r), \tag{1}$$

where r is the radial coordinate, a is the radius of the radiator, and U is the unit step function; $n = 0$, 1, and 2 correspond to the velocity profiles of rigid piston, simply supported and clamped radiators, respectively. V_{rms} denotes the rms velocity over the surface of the radiator given by

$$V_{rms} = \sqrt{\frac{1}{S}\int_S \mathrm{Re}\{v(r)\}^2 \mathrm{d}S} + i\sqrt{\frac{1}{S}\int_S \mathrm{Im}\{v(r)\}^2 \mathrm{d}S}, \tag{2}$$

where S is the area of the radiator. With this definition, V_{rms} is a complex number representing the phasor of the lumped membrane velocity and nonzero for all velocity profiles.

A radially symmetric velocity profile, $v(r)$, can be written in terms of the velocity profiles of (1) as

$$\begin{aligned} v(r) &= \alpha_1 v_1(r) + \alpha_2 v_2(r) + \cdots + \alpha_N v_N(r) \\ &= \sum_{n=0}^{N} \alpha_n v_n(r). \end{aligned} \tag{3}$$

The values of the coefficients, α_n, are calculated by first equating V_{rms} in each $v_n(r)$ to V of $v(r)$ resulting in

$$\begin{aligned} \alpha_0^2 + \sqrt{3}\alpha_0\alpha_1 + \cdots &= 1 \\ \sum_{n=0}^{N}\sum_{m=0}^{N} \frac{\sqrt{2n+1}\sqrt{2m+1}}{n+m+1}\alpha_n\alpha_m &= 1 \end{aligned} \tag{4}$$

and then using the least mean square algorithm with (4) to fit the velocity distribution to the actual one.

The velocity profile of a cMUT membrane depends on f/f_p, where f_p is the parallel resonance frequency[2] of the membrane. This profile determined by FEM simulations can be seen in Fig. 2 for $f = 0.2f_p$ and can be approximated using (3) with $\alpha_2 = 0.94$ and $\alpha_4 = 0.06$. The same figure also shows the velocity profiles of the membrane at $f = 0.4f_p$ with $\alpha_2 = 0.71$ and $\alpha_4 = 0.3$, and $f = f_p$ with $\alpha_2 = -2.45$ and $\alpha_4 = 3.06$, approximating the profiles very accurately. The variation of α_2 and α_4 is given in Table II as a function of f/f_p.

C. Radiation Impedance

The radiation impedance, Z, of a transducer with a velocity profile, $v(r)$, can be found by dividing the total power, P, at the surface of the transducer to the square of the absolute value of an arbitrary reference velocity, V [24], [25],

$$Z = \frac{P}{|V|^2} = \frac{\int_S p(r)v^*(r)\mathrm{d}S}{|V|^2}, \tag{5}$$

where $p(r)$ and $v^*(r)$ are the pressure and the complex conjugate of velocity at the radial distance r. All of the work on modeling the membranes since Mason [26] employ the average velocity, $V = V_{ave}$, to represent the lumped velocity variable. This choice is problematic with some higher mode cMUT velocity profiles, because it may give $V = 0$ [9] resulting in an infinite radiation impedance. In this work, the reference velocity is chosen to be the root mean square velocity, $V = V_{rms}$, defined above.[3]

[2] The parallel resonance frequency corresponds to the second circularly symmetric mode of the membrane.

[3] If this reference velocity is used in an electrical model of cMUT, the parameters of the model such as the transformer turns ratio, the capacitor, and the inductor at the mechanical side should be scaled by the factor $|V_{rms}|/|v_{ave}|$.

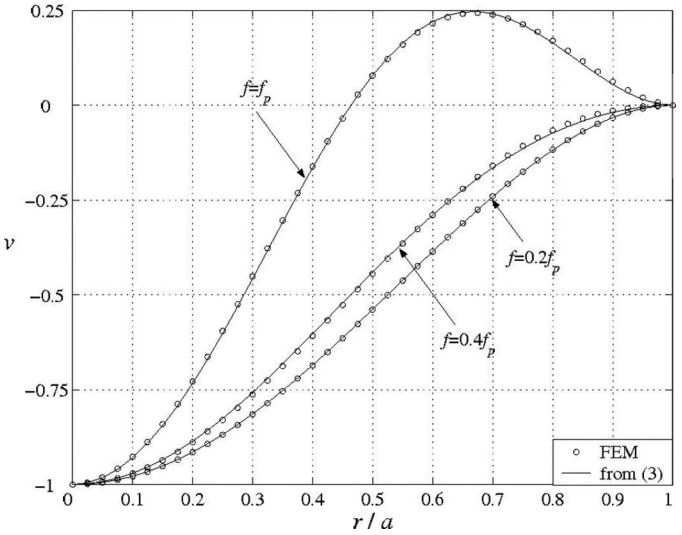

Fig. 2. The velocity profiles of a cMUT membrane normalized to the peak values determined by finite element method (FEM) simulations at $f = 0.2f_p$, $0.4f_p$, and f_p. The same profiles approximated using (3) with $[\alpha_2 = 0.94, \alpha_4 = 0.06]$, $[\alpha_2 = 0.71, \alpha_4 = 0.3]$, and $[\alpha_2 = -2.45, \alpha_4 = 3.06]$ are also shown.

For the velocity profile of (3), the total radiated power is

$$P = \int_S \sum_{n=0}^{N}\sum_{m=0}^{N} \alpha_n \alpha_m p_n(r) v_m^*(r) \mathrm{d}S = \sum_{n=0}^{N}\sum_{m=0}^{N} \alpha_n \alpha_m P_{nm}, \tag{6}$$

where P_{nm} is the power generated by $v_m(r)$ in the presence of the pressure field, $p_n(r)$ generated by $v_n(r)$. Following Greenspan [22], P_{nm} can be expressed in a closed form as

$$P_{nm} = S\rho_0 c_0 V_{\mathrm{rms}}^2 A\left\{1 - B\left[F_{1nm}(2ka) + iF_{2nm}(2ka)\right]\right\}, \tag{7}$$

where ρ_0 is the density of the medium and c_0 is the speed of the sound in the medium. Although A and B are constants, F_{1nm} and F_{2nm} are some functions of ka given in Table III for $n,m = 2$ and 4; k is the wavenumber in the immersion medium.

Using (3) with $n = 2$ and 4 and combining with (5), (6), and (7), Z is found as

$$Z = R + iX = \frac{\alpha_2^2 P_{22} + 2\alpha_2\alpha_4 P_{24} + \alpha_4^2 P_{44}}{|V_{rms}|^2}. \tag{8}$$

Here, R is the real part and X is the imaginary part of the radiation impedance. The real part is due to the real power radiated into the medium, whereas the imaginary part is due to the stored energy in the medium due to the sideways movements of the medium in close proximity of the membrane.

The radiation impedances computed from (8) and normalized by $S\rho_0 c_0$ for piston and clamped radiators (with velocity profiles given by (1) for $n = 0$ and $n = 2$) can be seen in Fig. 3 as a function of ka. As $ka \to \infty$, the mutual effects vanish and the normalized radiation resistance for both radiators converges to unity [27], [28]. For the same case, the radiators do not generate reactive power, hence,

TABLE I. MATERIAL PARAMETERS USED IN THE SIMULATIONS.

Parameter	Si_3N_4	Si	Water	Air
Young's modulus (GPa)	320	169		
Poisson's ratio	0.263	0.27		
Density (kg/m^3)	3270	2332	1000	1.27
Speed of sound (m/s)			1500	331

TABLE II. VARIATION OF α_2 AND α_4 WITH RESPECT TO f/f_p.

f/f_p	0	0.1	0.2	0.3	0.4	0.5	0.6	0.7	0.8	0.9	1
α_2	1	0.99	0.94	0.85	0.71	0.50	0.20	−0.23	−0.86	−1.64	−2.45
α_4	0	0.012	0.063	0.15	0.30	0.51	0.81	1.22	1.79	2.45	3.06

TABLE III. CONSTANTS AND FUNCTIONS USED IN (7).

n	m	A	B	$F_{1nm}(y)$	$F_{2nm}(y)$
2	2	1	$\frac{2^{11}\cdot 5}{(2ka)^7}$	$y^2J_5(y) + 2yJ_4(y) + 3J_3(y)$ $- y^3/16 - y^5/768$	$-y^2H_5(y) - 2yH_4(y) - 3H_3(y)$ $+ (2/\pi)\cdot(y^4/35) + (2/\pi)\cdot(y^6/945)$
2	4	$\frac{3\sqrt{5}}{7}$	$\frac{2^{17}\cdot 3\cdot 7}{(2ka)^{11}}$	$y^4J_7(y) + 5y^3J_6(y) + 27y^2J_5(y)$ $+ 105yJ_4(y) + 210J_3(y) - 35y^3/8$ $- y^7/(5.12\times 10^3) - y^9/(1.84\times 10^5)$	$-y^4H_7(y) - 5y^3H_6(y) - 27y^2H_5(y)$ $- 105yH_4(y) - 210H_3(y) + (2/\pi)\cdot(2y^4)$ $+ (2/\pi)\cdot(y^6/27) + (2/\pi)\cdot(2y^8/(3.47\times 10^3))$ $+ (2/\pi)\cdot(y^{10}/(1.34\times 10^5))$
4	4	1	$\frac{2^{23}\cdot 3^4}{(2ka)^{13}}$	$y^4J_9(y) + 4y^3J_8(y) + 18y^2J_7(y)$ $+ 60yJ_6(y) + 105J_5(y) - 7y^5/256$ $- y^7/(6.14\times 10^3) - y^9/(5.73\times 10^5)$ $- y^{11}/(3.30\times 10^7)$	$-y^4H_9(y) - 4y^3\ H_8(y) - 18y^2H_7(y)$ $- 60yH_6(y) - 105H_5(y) + (2/\pi)\cdot(y^6/99)$ $+ (2/\pi)\cdot(5y^8/(2.70\times 10^4)) + (2/\pi)\cdot(y^{10}/(4.05\times 10^5))$ $+ (2/\pi)\cdot(y^{12}/(3.45\times 10^7))$

J_n and H_n are the nth order Bessel and Struve functions.

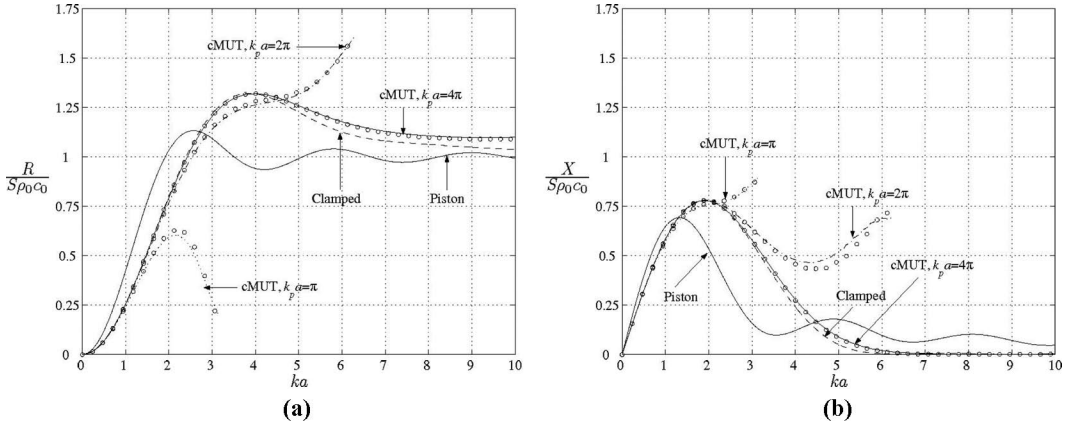

Fig. 3. The calculated radiation (a) resistance and (b) reactance normalized by $S\rho_0 c_0$ of a piston radiator, a clamped radiator, and cMUT membranes with $k_p a = \pi$, 2π, and 4π. The radiation impedances of the cMUT membranes determined by finite element method simulations (circles) are also included. The curves for cMUT membranes are shown for $ka \leq k_p a$.

the radiation reactances of both radiators approach zero. The figure also shows the normalized radiation impedances of 3 cMUT membranes with different $k_p a$ values as computed from (8), where k_p is the wavenumber at the parallel resonance frequency. The velocity profiles corresponding to different ka values are calculated from Table II using $ka/k_p a = f/f_p$ ratios. The frequencies less than the parallel resonance frequency of the cMUT membrane ($ka \leq k_p a$) are considered. cMUTs are similar to the clamped radiators for $ka < 0.4 k_p a$. In this range, the velocity profile of the cMUT membrane follows that of the clamped radiator. But, for $ka > 0.4 k_p a$, deviations from the clamped radiator behavior occur, especially when $k_p a$ is small and the mutual effects are significant. On the other hand, if $k_p a$ is high, the mutual effects are insignificant and R approaches that of the clamped radiator.

III. Radiation Impedance of an Array of cMUT Cells

A. Mutual Radiation Impedance Between Two cMUT Cells

If there are several transducers in the close proximity of the each other, one can define a mutual radiation impedance between them. The mutual radiation impedance, Z_{ij}, between ith and jth transducers is the power generated on the jth transducer due to the pressure generated by the ith transducer divided by the product of the reference velocities [25]

$$Z_{ij} = \frac{\int_{S_j} p_i(r_j) v_j^*(r_j) \mathrm{d}S}{V_i V_j^*} \quad i, j = 1, 2 \ldots, \quad i \neq j. \tag{9}$$

Using (3) with $n = 2$ and 4, Z_{ij} is found as

$$Z_{ij} = \alpha_2^2 Z_{ij}^{22} + 2\alpha_2 \alpha_4 Z_{ij}^{24} + \alpha_4^2 Z_{ij}^{44}, \tag{10}$$

where Z_{ij}^{nm} is the mutual radiation impedance between the transducers having the velocity profiles $v_n(r)$ and $v_m(r)$,

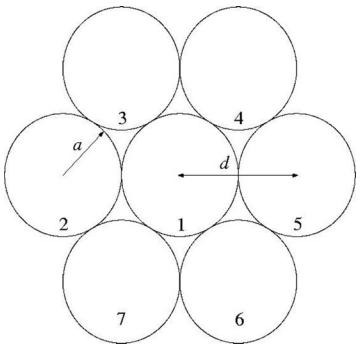

Fig. 4. The geometry of a circular array with hexagonally placed $N = 7$ cells and $d = 2\alpha$.

and it can be written as a double infinite summation with μ and v being the summation indices [21]

$$\begin{aligned} Z_{ij}^{nm} = {} & S\rho_0 c_0 \frac{2^{n+m} n! m! \sqrt{2n+1}\sqrt{2m+1}}{\sqrt{2kd_{ij}}(ka)^{n+m}} \\ & \times \sum_{\mu=0}^{\infty}\sum_{v=0}^{\infty} \left\{ \frac{\Gamma(\mu + v + 1/2)}{\mu! v!} \left(\frac{a}{d_{ij}} \right)^{\mu+v} \right. \\ & \times J_{\mu+n+1}(ka) J_{v+m+1}(ka) \\ & \left. \times \left[J_{\mu+v+1/2}(kd_{ij}) + i(-1)^{\mu+v} J_{-\mu-v-1/2}(kd_{ij}) \right] \right\}, \end{aligned} \tag{11}$$

where d_{ij} is the distance between ith and jth transducers.

B. Radiation Impedance of an Array of cMUT Cells

The calculation of the radiation impedance of an array of cMUT cells is demonstrated with an array, where equal size cells are placed in a hexagonal pattern giving the most compact arrangement [29]. Circular arrays as in Fig. 4 with $N = 7$, 19, 37, and 61 cells are investigated. The center-to-center spacing between neighboring cells is $d = 2a$ to use the area in the most efficient way. The radiation impedance of an N-cell array is modeled with

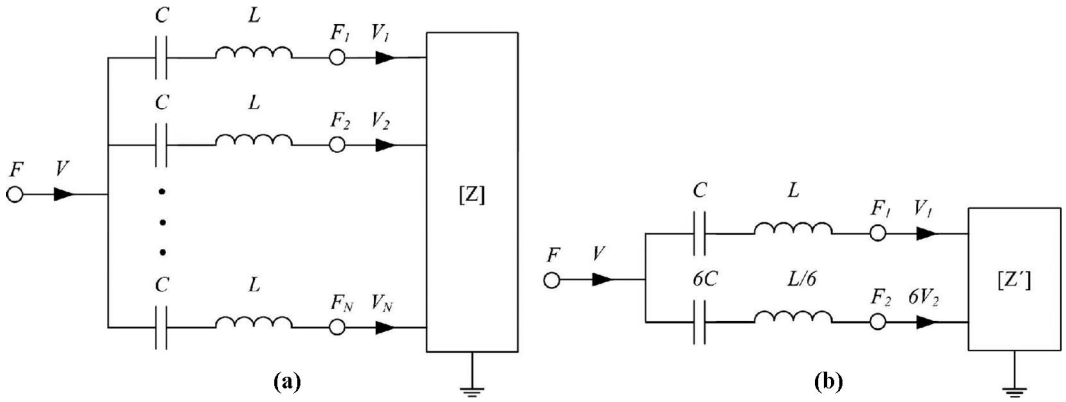

Fig. 5. The equivalent circuit of the radiation impedance for (a) a general array and (b) a circular array with hexagonally placed $N = 7$ cells.

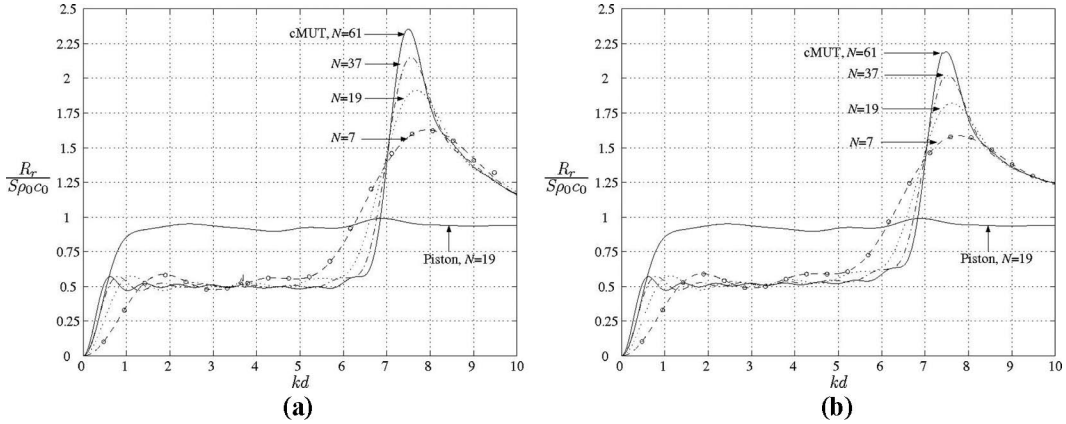

Fig. 6. The representative radiation resistance, R_r, normalized by $S\rho_0 c_0$ of a single cMUT cell in $N = 7$, 19, 37, and 61 element arrays in comparison to a cell in $N = 19$ element piston array all with $a/d = 0.5$ as a function of kd for a cMUT cell with (a) $k_p a = 2\pi$ and (b) $k_p a = 4\pi$. The representative radiation resistance determined by finite element method simulations (circles) is also shown.

an N-port linear network with a symmetrical $N \times N$ Z-parameter matrix where the diagonal elements are given by (8) and the off-diagonal elements are found from (10):

$$\begin{bmatrix} F_1 \\ F_2 \\ \vdots \\ F_N \end{bmatrix} = \begin{bmatrix} Z_{11} & Z_{12} & \dots & Z_{1N} \\ Z_{12} & Z_{11} & \dots & Z_{2N} \\ \vdots & \vdots & \ddots & \vdots \\ Z_{1N} & Z_{2N} & \dots & Z_{11} \end{bmatrix} \begin{bmatrix} V_1 \\ V_2 \\ \vdots \\ V_N \end{bmatrix}. \tag{12}$$

Here, F_i is the force and V_i is the lumped rms velocity at the ith cell as shown in Fig. 5(a). The LC section models the mechanical impedance of the membrane, Z_m [9]. Due to the symmetry, the 7-port network of a 7-cell array in Fig. 4 can be simplified to

$$\begin{bmatrix} F_1 \\ F_2 \end{bmatrix} = [Z'] \begin{bmatrix} V_1 \\ 6V_2 \end{bmatrix}, \tag{13}$$

where

$$[Z'] = \begin{bmatrix} Z_{11} & Z_{12} \\ Z_{12} & (Z_{11} + 2Z_{12} + 2Z_{24} + Z_{25})/6 \end{bmatrix} \tag{14}$$

because $Z_{12} = Z_{23} = Z_{27}$ and $Z_{24} = Z_{26}$. The resulting equivalent circuit is depicted in Fig. 5(b). Because the radiation impedance of each cell is different, we define a representative radiation impedance, Z_r, of a single cell as

$$Z_r = N\frac{F}{V} - Z_m = R_r + iX_r \tag{15}$$

where F and V are as shown in Fig. 5.

Fig. 6 shows the representative radiation resistance of a single cell normalized by $S\rho_0 c_0$ in various arrays as a function of kd for cMUT cells with $k_p a = 2\pi$ and 4π. For $kd < 5$, R_r of the cMUT cell shows a behavior similar to that of an array of pistons [17] except for the vertical scale. As kd increases, the positive loading on the each cell increases and R_r becomes maximum at around $kd = 7.5$, where the loading reaches an optimum point [28]. As N increases, the maximum value of radiation resistance, $R_{\max}$, also increases, although the corresponding kd value, kd_{opt}, is not significantly affected. On the other hand, as $kd \to \infty$, the mutual effects vanish and normalized value of R_r approach that of an individual cell. Note that for thin membranes with $k_p a < 3.7$, $kd_{\text{opt}} = 7.5$ point is beyond the parallel resonance frequency, hence, such a maximum will not be present.

The variation of $R_{\max}$ and kd_{opt} is investigated by changing the distance between the cells for an array with

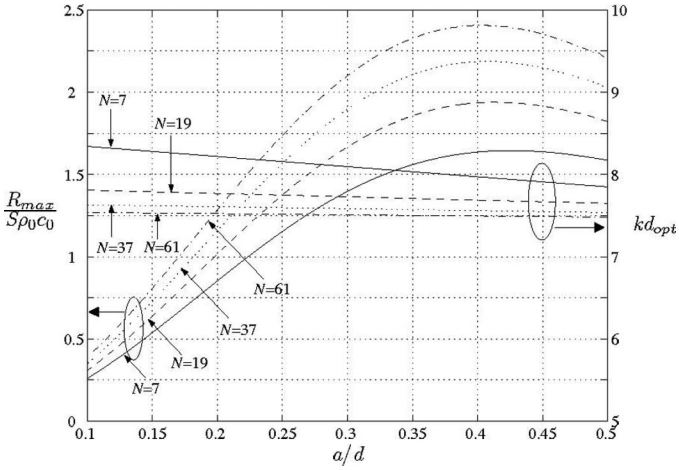

Fig. 7. kd_{opt} and normalized $R_{\max}$ as a function of a/d for a cMUT cell with $k_p a = 4\pi$ in $N = 7$, 19, 37, and 61 element arrays.

$k_p a = 4\pi$. The first peak in the radiation resistance and the corresponding kd value are taken as $R_{\max}$ and kd_{opt}, respectively. As depicted in Fig. 7, $a/d = 0.42$ and $kd_{\text{opt}} = 7.68$ define the optimum separation for $N = 19$. For example, at $f = 100$ kHz, this maximum for an airborne cMUT array is reached when $d = 4.05$ mm giving $a = 1.7$ mm. If the cMUT cell is made of a silicon membrane, then its thickness needs to be 69 μm [15] to have a mechanical resonance at 100 kHz. As shown in Fig. 7, there is only a 3% improvement in the radiation resistance by making $a/d = 0.42$ rather than the most compact arrangement of $a/d = 0.5$. Although this sparse arrangement results in a reduction in the fill factor [29] of about 30%, it may be necessary in fabricated arrays to leave space for anchors of the membrane; kd_{opt} varies between 7.5 and 8.3, and it is nearly independent of a/d as well as N.

In this work, the radiation impedance is calculated for the radially symmetric velocity profiles. The cMUT membrane has an antisymmetric mode at $0.54 f_p$ between the series and the parallel resonance frequencies [30]. In a dense medium like water, this mode can be excited depending on the position of the cell in the array [17]. This is most pronounced for the array with $N = 7$, because all the outer cells experience antisymmetric loading from the neighboring cells. To investigate this effect, the radiation impedance of an array made of cells with $d = 2.1a$, $k_p a = 2.15$ and 3.7 as determined by FEM simulations and calculated using (15) are plotted in Fig. 8(a).[4] For $k_p a = 2.15$, it is seen that there is a dip in the radiation resistance near $ka = 0.54 k_p a = 1.16$ (or $kd = 2.1 \times 1.16 = 2.4$) corresponding to the antisymmetric mode as determined from FEM simulations, which is not predicted by (15). The velocity profiles of the cells showing the excitation of antisymmetric mode at this frequency can be seen in Fig. 8(b). As

[4]For both curves, there is a wiggle around $0.25 k_p a$ predicted by analytic approach as well as FEM simulations. This point corresponds to the series resonance frequency of the membrane. The wiggle is due to the parallel combination of series RLC circuits with slightly different resonance frequencies. It does not exist for high $k_p a$ values, because the quality factor of RLC circuits is lower.

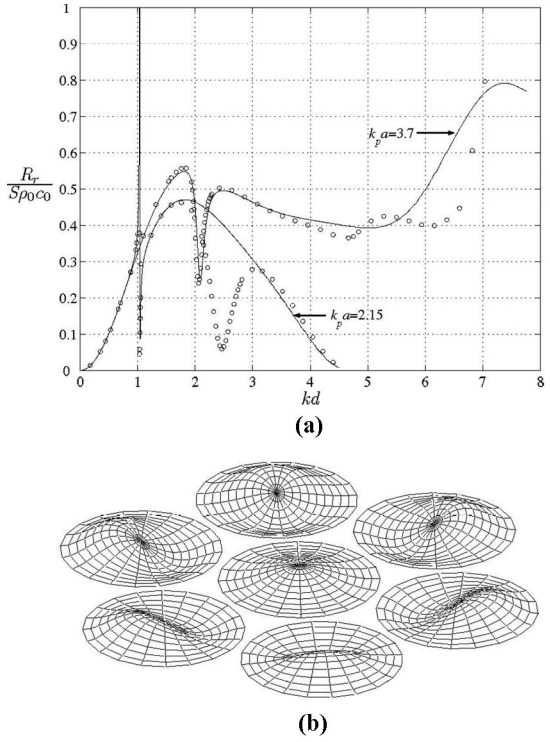

Fig. 8. (a) The representative radiation resistance normalized by $S\rho_0 c_0$ of a single cMUT cell in $N = 7$ element array in water for a cell with $d = 2.1a$, $k_p a = 2.15$ and 3.7. The representative radiation resistance determined by finite element method (FEM) simulations (circles) is also depicted. Note that the $k_p a = 2.15$ curve does not have the $kd_{\text{opt}} = 7.5$ peak. The discrepancy between FEM simulations and analytic curve is due to the presence of antisymmetric mode. (b) FEM computed velocity profile of the cells showing the excitation of antisymmetric mode at the outer cells for $k_p a = 2.15$ and $kd = 2.4$.

$k_p a$ increases, this effect is less pronounced. For $k_p a = 3.7$, the dip is still present near $kd = 2.1 \times 0.54 k_p a = 4.2$, but it is smaller. As seen in Fig. 6, the dip is nonexistent in thicker membranes with $k_p a = 2\pi$ or $k_p a = 4\pi$. Similarly, such dips are not present for airborne transducer arrays, because antisymmetric modes are not excited.

IV. Conclusions

The radiation impedance of a cMUT with a circular clamped membrane is calculated up to its parallel resonance frequency. The velocity profile of the membrane is written as a superposition of analytic velocity profiles whose weights are dependent on frequency. These profiles are used to calculate the individual and mutual radiation impedances from given expressions. Radiation impedance of any combination of cells can be found by considering only 2 cells at a time. Circular arrays are investigated to find the radiation resistances. It is found that the radiation resistance is a strong function of the separation of the cells. The center-to-center separation of the cells needs to be around $1.25\lambda_0$ ($kd = 7.8$) for a high radiation resistance. Note that the optimum cell separation may require a cMUT cell with an unusually large radius. With

an increased radius, the thickness of the membrane must also be increased to preserve the resonance at the operating frequency. In this case, the gap height may have to be reduced to keep the bias voltage at an acceptable level, because an increased membrane thickness implies a higher bias voltage. The model is perfectly valid for airborne applications. However, for thin membranes with $k_p a < 4$, the model may fail in water immersion around the antisymmetric mode.

References

[1] M. I. Haller and B. T. Khuri-Yakub, "A surface micromachined electrostatic ultrasonic air transducer," *IEEE Trans. Ultrason. Ferroelectr. Freq. Control*, vol. 43, pp. 1–6, Jan. 1996.

[2] I. Ladabaum, X. Jin, H. T. Soh, A. Atalar, and B. T. Khuri-Yakub, "Surface micromachined capacitive ultrasonic transducers," *IEEE Trans. Ultrason. Ferroelectr. Freq. Control*, vol. 45, pp. 678–690, May 1998.

[3] S. T. Hansen, A. S. Ergun, W. Liou, B. A. Auld, and B. T. Khuri-Yakub, "Wideband micromachined capacitive microphones with radio frequency detection," *J. Acoust. Soc. Am.*, vol. 116, pp. 828–842, 2004.

[4] I. O. Wygant, M. Kupnik, J. C. Windsor, W. M. Wright, M. S. Wochner, G. G. Yaralioglu, M. F. Hamilton, and B. T. Khuri-Yakub, "50 kHz capacitive micromachined ultrasonic transducers for generation of highly directional sound with parametric arrays," *IEEE Trans. Ultrason. Ferroelectr. Freq. Control*, vol. 56, pp. 193–203, Jan. 2009.

[5] O. Oralkan, A. S. Ergun, J. A. Johnson, M. Karaman, U. Demirci, K. Kaviani, T. H. Lee, and B. T. Khuri-Yakub, "Capacitive micromachined ultrasonic transducers: Next-generation arrays for acoustic imaging?" *IEEE Trans. Ultrason. Ferroelectr. Freq. Control*, vol. 49, pp. 1596–1610, Nov. 2002.

[6] D. M. Mills and L. S. Smith, "Real-time in-vivo imaging with capacitive micromachined ultrasound transducer (cMUT) linear arrays," in *Proc. IEEE Ultrasonics Symp.,* 2003, pp. 568–571.

[7] G. Caliano, R. Carotenuto, E. Cianci, V. Foglietti, A. Caronti, A. Iula, and M. Pappalardo, "Design, fabrication and characterization of a capacitive micromachined ultrasonic probe for medical imaging," *IEEE Trans. Ultrason. Ferroelectr. Freq. Control,* vol. 52, pp. 2259–2269, Dec. 2005.

[8] F. L. Degertekin, R. O. Guldiken, and M. Karaman, "Annular-ring cMUT arrays for forward-looking IVUS: Transducer characterization and imaging," *IEEE Trans. Ultrason. Ferroelectr. Freq. Control*, vol. 53, pp. 474–482, Feb. 2006.

[9] H. Köymen, M. N. Senlik, A. Atalar, and S. Olcum, "Parametric linear modeling of circular cMUT membranes in vacuum," *IEEE Trans. Ultrason. Ferroelectr. Freq. Control*, vol. 54, pp. 1229–1239, Jun. 2007.

[10] E. C. Wente, "A condenser transmitter as a uniformly sensitive instrument for the absolute measurement of sound intensity," *Phys. Rev.*, vol. 10, pp. 39–63, 1917.

[11] D. Stansfield, *Underwater Electroacoustic Transducers.* Bath, UK: Bath University Press and Institute of Acoustics, 1990.

[12] G. G. Yaralioglu, M. H. Badi, A. S. Ergun, and B. T. Khuri-Yakub, "Improved equivalent circuit and finite element method modelling of capacitive micromachined ultrasonic transducers," in *Proc. IEEE Ultrasonics Symp.*, 2003, pp. 469–472.

[13] A. Lohfink, P.-C. Eccardt, W. Benecke, and H. Meixner, "Derivation of a ID cMUT model from fern results for linear and nonlinear equivalent circuit simulation," in *Proc. IEEE Ultrasonics Symp.*, 2003, pp. 465–468.

[14] A. Bozkurt and M. Karaman, "A lumped circuit model for the radiation impedance of a 2D cMUT array element," in *Proc. IEEE Ultrasonics Symp.,* 2005, pp. 1929–1932.

[15] M. N. Senlik, A. Atalar, H. Koymen, and S. Olcum, "Radiation impedance and equivalent circuit for immersed cMUT array element," in *Proc. IEEE Ultrasonics Symp.*, 2006, pp. 1951–1954.

[16] A. Rønnekleiv, "cMUT array modeling through free acoustic cMUT modes and analysis of the fluid cMUT interface through fourier transform methods," *IEEE Trans. Ultrason. Ferroelectr. Freq. Control*, vol. 52, pp. 2173–2184, Dec. 2005.

[17] A. Caronti, A. Savoia, G. Caliano, and M. Pappalardo, "Acoustic coupling in capacitive microfabricated ultrasonic transducers: Modeling and experiments," *IEEE Trans. Ultrason. Ferroelectr. Freq. Control*, vol. 52, pp. 2220–2234, Dec. 2005.

[18] A. Bozkurt, I. Ladabaum, A. Atalar, and B. T. Khuri-Yakub, "Theory and analysis of electrode size optimization for capacitive microfabricated ultrasonic transducers," *IEEE Trans. Ultrason. Ferroelectr. Freq. Control*, vol. 46, pp. 1364–1374, Nov. 1999.

[19] Y. Roh and B. T. Khuri-Yakub, "Finite element modeling of capacitor micromachined ultrasonic transducers," in *Proc. IEEE Ultrasonics Symp.,* 2000, pp. 905–908.

[20] G. G. Yaralioglu, A. S. Ergun, and B. T. Khuri-Yakub, "Finite-element analysis of capacitive micromachined ultrasonic transducers," *IEEE Trans. Ultrason. Ferroelectr. Freq. Control*, vol. 52, pp. 2185–2198, Dec. 2005.

[21] D. T. Porter, "Self-and mutual-radiation impedance and beam patterns for flexural disks in a rigid plane," *J. Acoust. Soc. Am.*, vol. 36, pp. 1154–1161, 1964.

[22] M. Greenspan, "Piston radiator: Some extensions of the theory," *J. Acoust. Soc. Am.*, vol. 65, pp. 608–621, 1979.

[23] I. O. Wygant, M. Kupnik, and B. T. Khuri-Yakub, "Analytically calculating membrane displacement and the equivalent circuit model of a circular cMUT cell," in *Proc. IEEE Ultrasonics Symp.,* 2008, 2111–2114.

[24] L. L. Foldy, "Theory of passive linear electroacoustic transducers with fixed velocity distribution," *J. Acoust. Soc. Am.*, vol. 21, pp. 595–604, 1949.

[25] H. Sherman, "Analysis of acoustic interactions in transducer arrays," *IEEE Trans. Sonics Ultrason.*, vol. 13, pp. 9–15, 1966.

[26] W. P. Mason, *Electromechanical Transducers and Wave Filters*, 2nd ed. New York: D. Van Nostrand Company, Inc., 1948.

[27] D. T. Blackstock, *Fundamentals of Physical Acoustics.* New York: John Wiley & Sons, Inc., 2000.

[28] H. Lee, J. Tak, W. Moon, and G. Lim, "Effects of mutual impedance on the radiation characteristics of transducer arrays," *J. Acoust. Soc. Am.*, vol. 115, pp. 666–679, 2004.

[29] R. L. Pritchard, "Mutual acoustic impedance between radiators in an infinite rigid plane," *J. Acoust. Soc. Am.*, vol. 32, pp. 730–737, 1960.

[30] A. Leissa, *Vibration of Shells.* Washington, D.C.: NASA, 1969.

Muhammed N. Senlik was born in Isparta, Turkey, in 1981. He received his B.S. and M.S. degrees from Bilkent University, Ankara, Turkey, in 2002 and 2005, respectively, both in electrical and electronics engineering. He is about to finish his Ph.D. study at Bilkent University in the Electrical and Electronics Engineering Department.

Selim Olcum was born in Chicago, IL, in 1981. He received his B.S. and M.S. degrees in electrical engineering in 2003 and 2005, respectively, both from Bilkent University, Ankara, Turkey.

He worked as a guest researcher at National Institute of Standards and Technology, Semiconductor Electronics Division, Gaithersburg, MD, during the summers of 2002 and 2003. He was a visiting scholar in Micromachined Sensors and Transducers Laboratory of the Georgia Institute of Technology, Atlanta, GA, in 2006. He is currently working toward his Ph.D. degree in the Electrical and Electronics Engineering Department at Bilkent University, where he has been a research and teaching assistant since 2003.

His current research interests include optical and acoustical micromachined sensors and actuators.

Mr. Olcum is a recipient of the ASELSAN Ph.D. Scholarship. He has been a member of IEEE and the UFFC Society since 2003.

Hayrettin Köymen received the B.Sc. and M. Sc. degrees from Middle East Technical University (METU), Ankara, Turkey, in 1973 and 1976, respectively, and the Ph.D. degree from Birmingham University, Birmingham, UK, in 1979, all in electrical engineering.

He worked as a faculty member in the Marine Sciences Department (Mersin) and Electrical Engineering Department (Ankara) of METU, from 1979 to 1990, and in Bilkent University, Ankara, Turkey, since 1990, where he is a professor. His research activities have included underwater acoustic and ultrasonic transducer design, acoustic microscopy, ultrasonic NDT, biomedical instrumentation, mobile communications, and spectrum management.

Dr. Köymen is a fellow of IET (formerly IEE).

Abdullah Atalar received his B.S. degree from Middle East Technical University, Ankara, Turkey, in 1974, and his M.S. and Ph.D. degrees from Stanford University, Stanford, CA, in 1976 and 1978, respectively, all in electrical engineering. From 1978 to 1980, he was first a postdoctoral fellow and later an engineering research associate at Stanford University. For 8 months, he was with Hewlett Packard Labs, Palo Alto, CA. From 1980 to 1986, he was on the faculty of the Middle East Technical University as an assistant professor. In 1986, he joined Bilkent University, Ankara, Turkey, as chairman of the Electrical and Electronics Engineering Department and served in the founding of the department, where he is currently a professor. He is presently the provost of Bilkent University. From 1986 to 1998, he was a visiting professor at Stanford University. His current research interests include microwave electronics and micromachined sensors. He was awarded the Science Award of the Turkish Scientific Research Council (TUBITAK) in 1994. He is a fellow of IEEE and a member of Turkish Academy of Sciences.